

*Article*

## Silver Nanoparticles/Skim Natural Rubber/Bacterial Cellulose Biopolymer Film

Puttakhun Meemai<sup>1</sup>, Theerapart Sripetchdanon<sup>1</sup>, Nuntaporn Laosarakham<sup>1</sup>, Saranrat Siri<sup>1</sup>, Adun Nimpaiboon<sup>2</sup>, and Muenduen Phisalaphong<sup>1,\*</sup>

<sup>1</sup> Bio-Circular-Green-economy Technology & Engineering Center (BCGeTEC), Department of Chemical Engineering, Faculty of Engineering, Chulalongkorn University, Bangkok, 10330, Thailand

<sup>2</sup> Rubber Technology Research Centre (RTEC), Faculty of Science, Mahidol University, Nakhon Pathom 73170, Thailand

\*E-mail: muenduen.p@chula.ac.th (Corresponding author)

**Abstract.** The accumulation of non-degradable wastes is a significant threat to ecosystems and living organisms, necessitating urgent action to mitigate their environmental impact. This paper presents the synthesis and fabrication of green and biodegradable composite films with antimicrobial properties from silver nanoparticles, skim natural rubber (SNR), and bacterial cellulose (BC). BC was cultivated using organic agricultural waste and then was modified through immersion in silver nanoparticles synthesized within SNR latex. Characterizations of BC-SNR-Ag biopolymeric composites such as silver nanoparticle dispersion, mechanical strength, thermal stability, water absorption capacity and antibacterial properties were investigated. The results showed that the concentration of silver nitrate influenced the production and the diffusion of silver particles into the BC matrix. Furthermore, compared to pure BC film, the inclusion of SNR and silver nanoparticles significantly enhanced the properties of the composites in terms of flexibility and antibacterial properties.

**Keywords:** Silver nanoparticles, natural rubber, bacterial cellulose, flexibility materials.

ENGINEERING JOURNAL Volume 28 Issue 10

Received 7 June 2024

Accepted 1 October 2024

Published 31 October 2024

Online at <https://engj.org/>

DOI:10.4186/ej.2024.28.10.13

## 1. Introduction

Nowadays, non-degradable waste has become a significant problem. On the other hand, utilizing biodegradable materials synthesized from natural polymers offers many benefits [1, 2]. These biodegradable materials, derived from renewable sources such as plants or microorganisms, possess the ability to break down naturally over time, reducing environmental pollution and waste accumulation. By replacing plastic with alternative biodegradable materials for various products and packaging, we can mitigate the environmental impact of non-degradable waste and change towards a more sustainable future [3]. The use of biodegradable materials encourages the development of eco-friendly alternatives in industries ranging from packaging to textiles and beyond, contributing to the global efforts towards environmental conservation and waste reduction.

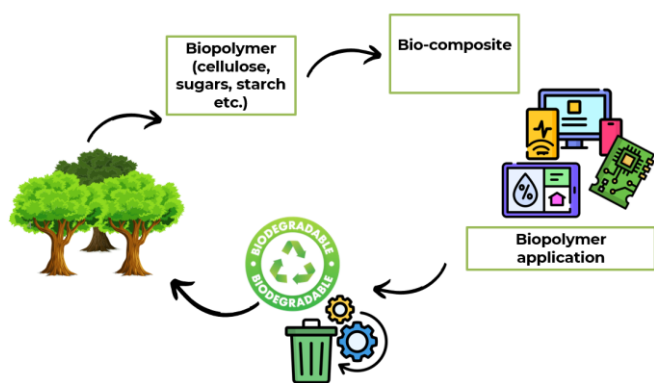


Fig. 1. The life cycle of biopolymers to electronic devices.

Biopolymers have received widespread attention due to growing concerns about the increase in plastic waste from fossil sources, which cannot biodegrade naturally. Biopolymers produced by plants or microorganisms tend to biodegrade naturally when exposed to bacteria in soil or seafloor sediments [4]. Commonly used biopolymers include natural rubber, starch, and cellulose, with other materials like chitosan gaining significant interest [5]. However, many natural polymers exhibit poor mechanical properties and relatively low chemical resistance compared to synthetic polymers [6]. To enhance the properties of biopolymers, research has focused on adding fillers or blending them with other polymers to improve their mechanical strength, chemical resistance, and overall functionality. Bacterial cellulose (BC) stands out as a valuable and eco-friendly material due to its biodegradability, renewable nature, and versatility in various applications. Produced by bacteria like *Gluconacetobacter xylinus*, BC can be synthesized using waste materials, reducing environmental pollution and offering a sustainable alternative to traditional biomaterials [7]. Its production process is energy-efficient and emits fewer greenhouse gases compared to plant cellulose extraction, further enhancing its environmental credentials [8].

Bacterial cellulose (BC) is a versatile biomaterial with exceptional properties such as high purity, mechanical strength, biocompatibility, and a porous nano-fibrillar 3D structure [9–11]. However, BC lacks inherent antimicrobial properties, and its stress-bearing capacity is hindered by numerous pores, despite its high mechanical properties. BC demonstrates significant potential as both a matrix and reinforcement in composite materials due to its structural characteristics. Recent researches have focused on synthesizing different types of BC composites, resulting in enhancements in mechanical, biological, and electrical properties [12]. Various methods have been explored to improve BC properties, including modifications to synthesis techniques and culture conditions, as well as incorporating BC with other materials to create diverse BC composites. These advancements aim to expand the application of BC across various fields. To address this, fillers are often incorporated to enhance their mechanical strength, electrical conductivity, and other functional properties [13]. These modifications significantly expand the potential applications of BC, providing the necessary enhancements to meet diverse performance requirements [14].

Natural rubber latex (NRL) is a colloidal dispersion containing cis-1,4 Polyisoprene, extracted from the notched bark of *Hevea-Brasilensis* trees in the form of a white and milky fluid. Fresh NRL typically comprises 30–40% rubber particles, 5–10% non-rubber components, and 55–65% water (Table 1) [15, 16]. Natural rubber (NR) is well-known for its remarkable flexibility, strength, and elasticity, making it a highly sought-after material. It exhibits resistance to water and certain chemicals, adding to its versatility in various applications. The distinctive elastic property of NR is from the loosely bound isoprene chains, which can reattach themselves when pulled apart, ensuring resilience and durability. Additionally, NR boasts several notable characteristics, including excellent tear strength, moderate resistance to light, heat, and ozone, and high resilience against tearing, chopping, and cutting. These inherent properties make natural rubber a valuable fillers across a wide range of applications [17, 18]. Skim natural rubber (SNR) is a low-cost by-product produced during concentrated latex production. Fresh natural rubber (FNR) consists of rubber particles with a core of cis-1,4-polyisoprene, surrounded by proteins and phospholipids. To prevent coagulation and decay after tapping, ammonia (NH<sub>3</sub>) is added to stabilize the latex and inhibit bacterial growth. During centrifugation, FNR is separated into concentrated latex with about 60% dry rubber content (DRC) and SNR, which has 4–7% DRC and some residual ammonia [17, 19]. The rubber industry plays a crucial role in Thailand's economy, with policies aimed at increasing domestic rubber utilization and processing, which can elevate the value of SNR [20, 21]. While traditionally used in low-cost products, SNR's incorporation into BC can provide advantageous properties and enhance its applications.

Table 1. Component of fresh natural rubber latex [1].

Constituent	Content (%)
Rubber particles	30-40
Water	55-65
Proteins	2-3
Lipids	0.1-0.5
Sugars	1-2
Ash	0.5-1
Others	1.5-3.5

Previously, the reinforcement of BC with SNR latex resulted in significant improvements in mechanical strength, structural stability, and dielectric properties of the composite films [17]. Notably, SNR diffuses extensively into the BC network, resulting in considerably higher loading than those loading by using fresh natural rubber (FNR). The modified films exhibit excellent resistance to chemicals, biodegradability, and improved dielectric properties, making this composite promising for electronic applications [17]. SNR plays an important role in the mechanical properties of composite film. SNR is rich in small rubber particles and proteins. Incorporating SNR into BC films increases the strain at break, making the composite films more stretchable and flexibility; however, it causes the reduction in tensile modulus. Additionally, organic substance (OGS) or residual ammonia in the SNR latex could form a complex with the silver ions, which then reacted with reducing agents such as glucose and other organic compounds present in the latex. Proteins in the latex also acted as stabilizing agents, promoting silver particle growth.

Metal nanoparticle can be synthesized through physical and chemical methods [22]. Silver nanoparticles have been widely used as a filler incorporated into polymers. The most commonly employed method for silver particle synthesis is chemical reduction [23]. Silver nanoparticles could be synthesized by the green synthesis method using SNR. Ammonia, left over from processing, forms complexes with silver ions. Glucose, a natural reducing agent, donates electrons to convert these silver ions into nanoparticles. Proteins in the latex act as stabilizing agents, capping the nanoparticles to prevent aggregation and ensure uniformity. Additionally, other organic compounds, including amino acids and various sugars may also contribute to the reduction and stabilization processes [24]. Danwanichakul et al. synthesize silver nanoparticles in SNR latex by using NR as a reducing agent [25]. Suwatthanarak et al. also synthesized silver nanoparticles in SNR latex using silver nitrate, ammonia, glucose, and BSA proteins and reducing agents. The type and concentration of applied reducing agents affect number and size of silver particles [24].

This research aims to develop a novel procedure for synthesis and fabrication biopolymer composite films of BC, SNR and silver particles (BC-SNR-Ag). The BC-SNR-Ag composites were characterized in terms of morphology, mechanical and thermal properties, water

absorption and antibacterial properties to guide for further applications.

## 2. Materials and Experimental

### 2.1. Materials

Table 2. Experimental materials.

Material	Manufacturer	Specification
Silver nitrate (AgNO <sub>3</sub> )	RCI Labscan Ltd. (Bangkok, Thailand)	purity, >99.8%
Ammonium sulfate	RCI Labscan Ltd. (Bangkok, Thailand)	-
Acetic acid	Mallinckrodt Chemicals (Paris, KY, USA)	-
Sodium hydroxide (NaOH)	Ke-maus (New South Wales, Australia).	-
Skim natural rubber	Rubber Technology Research Centre (RTEC) (Nakhon Pathom, Thailand)	-
Mature coconut water	Burapha City Bang Wua Fresh Market, (Chachoengsao, Thailand)	-
<i>Gluconacetobacter xylinus</i>		Bacterial strain AGR 60

### 2.2. Bacterial Cellulose Cultivation

BC pellicles were synthesized using mature coconut water, a low-cost byproduct from the coconut milk industry. Utilizing mature coconut water as the primary culture medium for BC production can reduce production costs. The medium was prepared by mixing coconut water with 0.5% (w/v) ammonium sulfate, 5.0% (w/v) sucrose, and 1.0% acetic acid solution (30%, v/v), then sterilizing it at 110°C for 5 minutes. Pre-cultures were established by transferring 15 mL of a *Gluconacetobacter xylinus* stock culture into 300 mL of the medium in a 500 mL Erlenmeyer flask and incubating statically at 30°C for 7 days. Subsequently, 60 mL of the sterile medium was combined with 3 mL of the pre-culture broth in a sterile petri dish and incubated statically at 30°C for 7 days. The resulting BC pellicles were

purified by washing with deionized water (DI) for 30 minutes, treating with 1% (w/v) sodium hydroxide solution at room temperature for 24 hours to remove bacterial cells, washing with running water for 30 minutes, and then rinsing with DI water until the pH was neutral [26].

### 2.3. Silver Nanoparticles Synthesis

Silver nanoparticles (AgNPs) were synthesized by using a green method, employing organic compounds in SNR as reducing agent. The solution of silver nitrate ( $\text{AgNO}_3$ ) was employed as the silver source for the reduction reaction. AgNPs were produced in cost-effective SNR latex. Organic substance (OGS) or residual ammonia in the latex formed a complex with the silver ions, which then reacted with reducing agents such as glucose and other organic compounds present in the latex. Proteins in the latex acted as stabilizing agents, promoting particle growth [21].

Silver nanoparticles were synthesized via in situ reduction of  $\text{AgNO}_3$  to metallic silver nanoparticles (AgNPs). Various concentrations of  $\text{AgNO}_3$  solution (40, 80, 120, and 160 mM) were used in this study. The solution of  $\text{AgNO}_3$  was prepared by dissolving  $\text{AgNO}_3$  in deionized water. The suspension of SNR (8% by weight of dry rubber content) was heated to  $80^\circ\text{C}$  under constant mechanical stirring at 500 rpm. Subsequently, 5 mL of  $\text{AgNO}_3$  solution was added to the prepared SNR suspension. The suspensions of AgNPs/SNR were stirred and maintained at  $80^\circ\text{C}$  for 8 hours.

### 2.4. Preparation of Bio-Polymeric Film

AgNPs/SNR/BC (Ag-NB) films were prepared using the immersion method. Purified BC pellicles were rinsed with deionized water for 5 minutes. The AgNPs/SNR suspension was poured into a 14.5 cm diameter glass petri dish. A piece of BC was immersed in 30 mL of the suspension and incubated at  $80^\circ\text{C}$  for 48 hours in an air-circulating oven to ensure the extensive diffusion of AgNPs and SNR into the BC matrix. The resulting composite films were washed with 250 mL deionized water for 5 minutes to remove excess components, followed by air drying for 24 hours to eliminate residual moisture. The composite films were stored in an airtight container prior to characterization and further application.

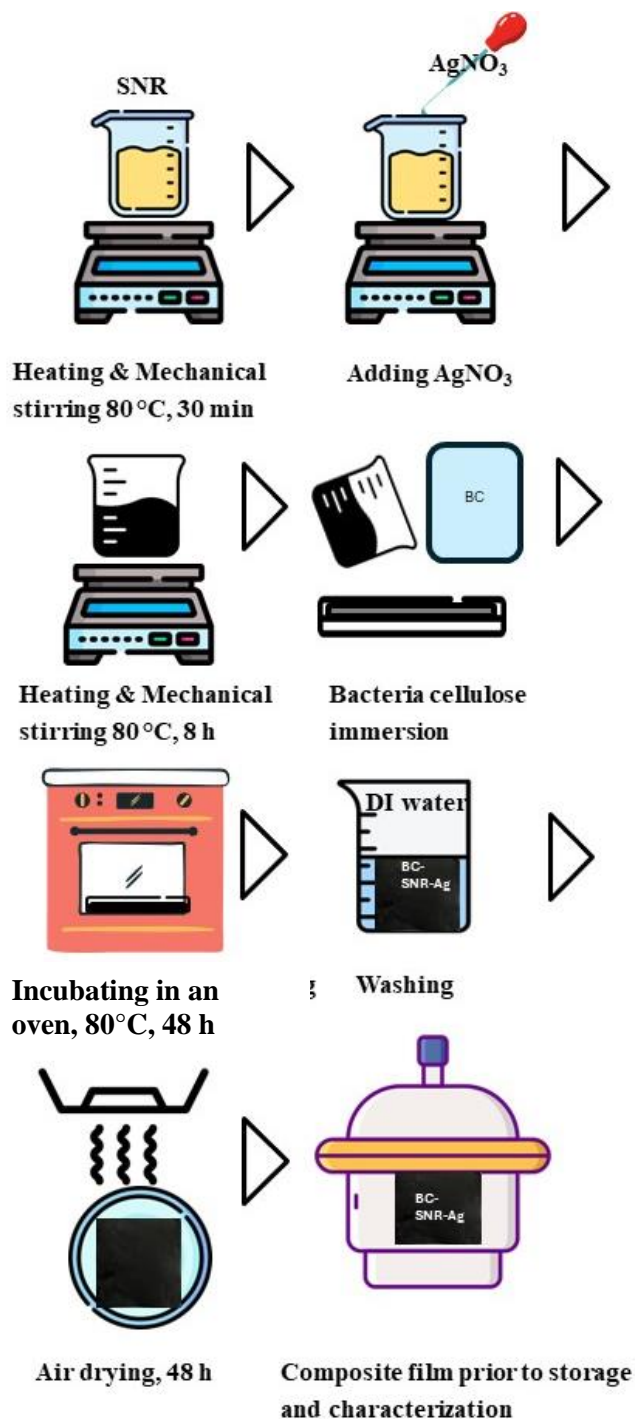


Fig. 2. Schematic depicting the synthesis method of BC-SNR-Ag composites.

### 2.5. Characterization of Composites

The morphologies of the BC and BC composites were examined using a Field Emission Scanning Electron Microscope (FE-SEM, Thermo Fisher Scientific, Quanta 250 FEG, Hillsboro, OR, USA) coupled with an energy dispersive X-ray spectrometer. The specimens were sputter-coated with gold, and the SEM-EDS analyses were conducted at an accelerating voltage ranging from 5 to 15 kV.

Residual weight analysis was carried out using a thermogravimetric analyzer (TGA, NETZSCH TG 209 F3 Tarsus, Germany). Film samples weighing between 3

to 8 mg were heated from 25 to 800 °C at a constant rate of 15 °C/min under a nitrogen atmosphere.

The water adsorption capacity was measured by immersing the dry sample in DI water at room temperature (28°C) until it reached equilibrium. The initial weights of the dry samples were recorded as  $W_d$ . After being immersed in the DI water, Kimwipes papers were used to remove excess water from samples. Weight of the wet samples was inscribed as  $W_h$ . The WAC was calculated using the following formula.

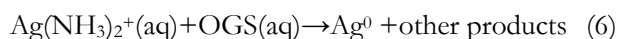
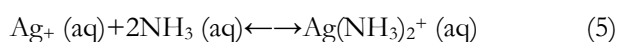
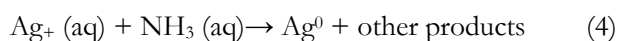
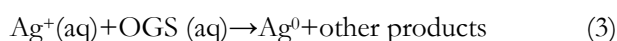
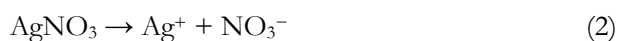
$$\text{WAC (\%)} = (W_h - W_d) / W_d \times 100 \quad (1)$$

The mechanical properties of dry films, including Young's modulus, tensile strength, and elongation at break for BC and BC-Ag composites, were evaluated according to the ASTM D882 (2004) standard. These tests were performed using a Universal Testing Machine (Hounsfield H10 KM, Redhill, England), with the samples prepared as rectangular film sheets measuring  $1 \times 2.5 \text{ cm}^2$ . Five specimens for each sample type were tested to calculate the average value and the standard deviation. The tests were conducted at a speed rate of 10 mm/min, a standard rate that balances precision and practicality in measuring mechanical properties.

### 3. Results and Discussion

#### 3.1. Silver Nanoparticles Synthesis

The synthesis of silver nanoparticles (AgNPs) was successfully achieved without the use of any other reducing agents or stabilizers [24, 25] as follows:



Ammonia, being more prevalent, can promote the reactions. The nitrate in Eq. (2) would react with the reducing agent, an organic substance (OGS) within SNR latex Eq. (3). Ammonia also acts as a reducing agent and can directly form a complex ion with  $\text{Ag}^+$  Eq. (4). These complex ions can behave as an oxidizing agent and react with organic substances to produce  $\text{Ag}^0$ . Subsequently,  $\text{Ag}^0$  would aggregate into larger particles, known as AgNPs (Eq. (6), (7), and (8)) [25].

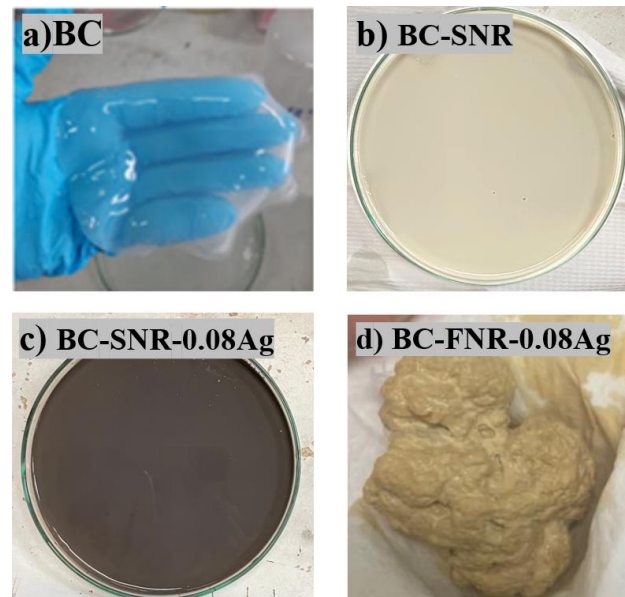


Fig. 3. Picture of (a) BC, (b) BC-SNR, (c) BC-SNR-0.08Ag, (d) BC-FNR-0.08Ag.

In the preliminary study, AgNPs were synthesized in both fresh natural rubber (FNR) latex and skim natural rubber (SNR) latex. However, by synthesizing AgNPs in FNR latex, the NR particles tended to agglomerate and form clusters after the reactions (Fig. 3(d)). The leftover ammonium was trapped into FNR clusters and later caused oxidative degradation and polymer chain scission. This ongoing chemical activity leads to product degradation, ultimately causing BC-FNR-Ag composites to decompose [25]. However, no such problem was observed by using SNR latex. Additionally, the addition of the solution of  $\text{AgNO}_3$  to SNR latex changes the suspension color to a darker brown (Fig. 3(c)). This color change indicated the synthesis of AgNPs. According to the result of the preliminary study, the procedure for the synthesis of AgNPs was performed only in SNR latex for further study.

#### 3.2. Fabrication of Composites

On Fig. 4 (left side), the introduction of AgNPs and SNR into BC matrix led to rougher surfaces due to the dispersion and accumulation of AgNPs and NR particles on surface [27]. Considering the cross-section views (Fig. 4, right side), each composite film demonstrated thorough dispersion of SNR into BC matrix without phase separation. SNR was well incorporated into the cellulose fibril network and filled the pores, while AgNPs were dispersed in the form of very small particles in SNR matrix. Only some small portions of AgNPs were observed from the FE-SEM images as shown in Fig. 4.

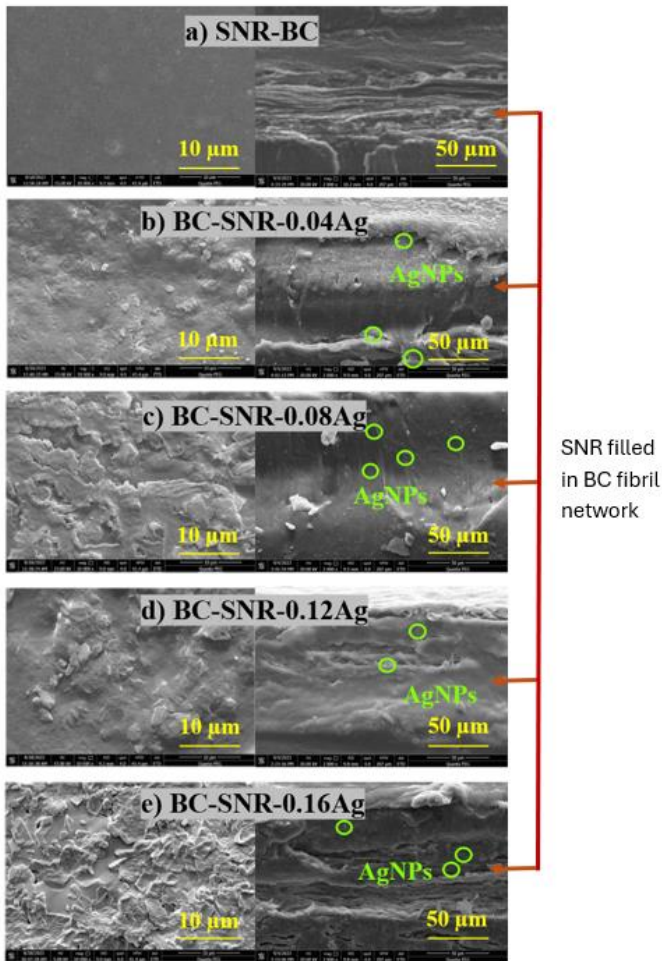


Fig. 4. FE-SEM images of dried composite films: surface area (left) and cross section (right) of (a) BC-SNR, (b) BC-SNR-0.04Ag, (c) BC-SNR-0.08Ag, (d) BC-SNR-0.12Ag, and (e) BC-SNR-0.16Ag, showing AgNPs dispersed in SNR, which filled in BC fibril networks.

The good distribution of AgNPs in the composite films could be clearly observed from the EDX mapping (Fig. 5, left), in which the estimated average sizes (using ImageJ) of AgNPs in the films of BC-SNR-0.04Ag, BC-SNR-0.08Ag, BC-SNR-0.12Ag and BC-SNR-0.16Ag were  $0.196 \pm 0.019$ ,  $0.201 \pm 0.020$ ,  $0.218 \pm 0.029$ , and  $0.225 \pm 0.028$   $\mu\text{m}$ , respectively. The increase in the concentration of  $\text{AgNO}_3$  led to a corresponding increase in AgNP size, attributed to a greater number of nucleation events which facilitated the growth of larger nanoparticles [28]. Additionally, the higher metal concentration promoted nanoparticle aggregation, driven by electrostatic interactions and van der Waals forces, resulting in the formation of larger agglomerates [29].

The increase in  $\text{AgNO}_3$  concentration resulted in the higher formation of AgNPs. However, only a slight increase in Ag content in films was obtained from changing the  $\text{AgNO}_3$  concentration from 120 mM to 160 mM (Fig. 5, right). As the concentration of  $\text{AgNO}_3$  increases, Ag particles grow in size, making their diffusion into the BC matrix more challenging. Consequently, despite the higher concentration of AgNPs in SNR

suspension, due to the reduced penetration of larger nanoparticles into the cellulose structure, there was not much difference in Ag weight percent between BC-SNR-0.16Ag and BC-SNR-0.12Ag. In the comparison of Ag weight percents obtained by the EDX mapping and TGA analysis, it indicated that the concentration of AgNPs in the outer part was remarkably higher than that in the inner part. Due to the limitation in mass transfer, the diffusion of AgNPs into the BC matrix might be restricted. The diffusional limitation could lead to a lower concentration of AgNPs in the inner part of the composite films. As the particle size was larger, the diffusion of the particles into the inner part of the films should be more limited.

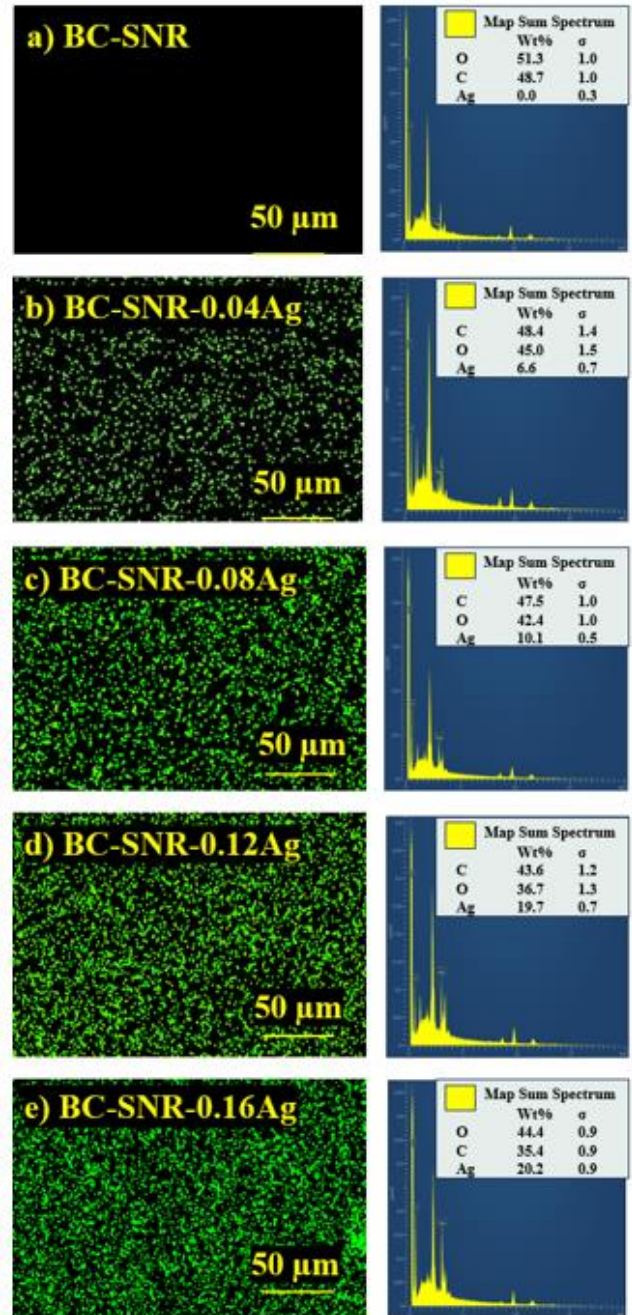


Fig. 5. EDX elemental mapping analysis of Ag and map sum spectrum of the composite films: (a) BC-SNR, (b) BC-SNR-0.04Ag, (c) BC-SNR-0.08Ag, (d) BC-SNR-0.12Ag, and (e) BC-SNR-0.16Ag,

### 3.3. Mechanical Properties

The mechanical properties of pure BC film in terms of tensile modulus, tensile strength and strain at break were 11,201 MPa, 107.03 MPa, and 1.48%, respectively. The mechanical properties of BC-SNR-Ag composite films, reinforced with varying amounts of AgNPs in SNR, are shown in Fig. 6. As compared to pure BC film [17], the incorporation of SNR considerably improved the elasticity and flexibility of the composite films as shown in the values of strain at break (Fig. 6(c)). The BC-SNR-Ag composite exhibited higher strain at break, but lower tensile strength and modulus as compared to pure BC film. The incorporation of NR into the BC networks resulted in the ability of the fibers to absorb more energy and could prevent the nanocellulose fibers from breaking and make it more flexibility [30]; however, it resulted in lower tensile strength and modulus of the films. This substantial improvement makes the composites more suitable for flexible applications. As compared to BC-SNR film, the incorporation of AgNPs into films caused a significant decrease in strain at break because the inclusion of highly crystalline AgNPs in films could trigger the higher rigidity and stiffness of the materials [30]. On the other hand, the tensile strength of BC-SNR-Ag remains rather constant comparable to BC-SNR, while the tensile modulus decreases with addition of AgNPs, which might be due to AgNPs acting as impurities within the BC-SNR matrix, leading to a decrease in the tensile modulus of the composite polymer [31].

### 3.4. Thermal Properties

The film of BC-SNR-Ag was analyzed for thermal stability. The TGA curve illustrates the thermal degradation profiles composite as shown in Fig. 7. Due to its overall good morphologies and mechanical properties, BC-SNR-0.08Ag was selected as a composite film sample for the characterization. The results reveal several stages of thermal degradation. The first stage, involving minor weight loss, occurred between room temperature and 150°C, attributed to the evaporation of residual water in the film. The second stage, showing significant weight loss, occurs between 280°C and 370°C and was attributed to cellulose degradation. The final stage, with a small weight loss observed between 400°C and 800°C, corresponded to the degradation of carbonaceous residues [32]. Thermal stability is essential for electronic materials and many applications, as it affects both their processing and their effectiveness in high-temperature environments. The addition of AgNPs enhances the residual mass as compared to that of BC-SNR. The weight residue percentages for BC-SNR was 13.92%, while NR experienced a total weight loss of approximately 99.63%, which indicated nearly complete degradation due to its poor thermal resistance [10, 33]. The TGA curve of BC-SNR-0.08Ag demonstrated improved thermal stability, retaining approximately 18.86% of its weight at temperatures as high as 800°C. The incorporation of

AgNPs in the films could enhance the thermal stability of the film owing to the high heat stability of AgNPs [31].

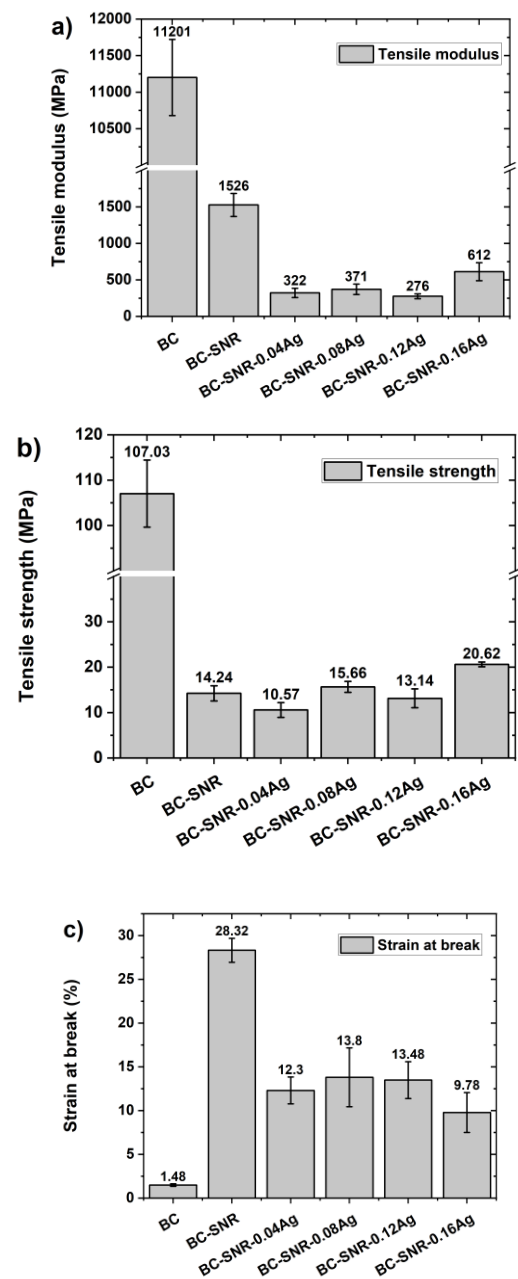


Fig. 6. Tensile modulus (a), Tensile strength (b), and Strain at break (c) of BC-SNR-Ag composites.

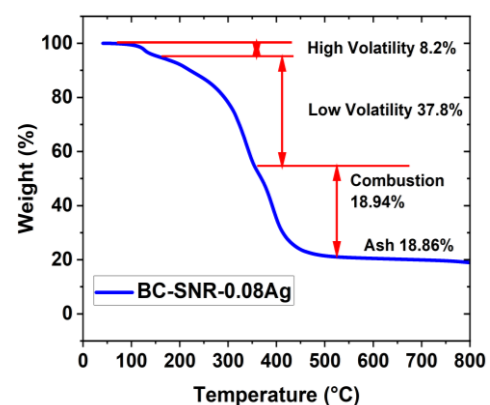


Fig. 7. TGA curves of BC-SNR-0.08Ag.

From the TGA results, the weight residue of BC-SNR was 13.92%, while the weight residue of BC-SNR-AgNPs was 18.86%. The difference in weight residue was estimated to be the weight of AgNPs, which was around 4.9%, which was different from Ag weight percent reported from EDX. The EDX mapping of elements on the film provides the elemental details of near surface elements of a sample. The result from the EDX mapping of Ag on BC-SNR-0.08 Ag film revealed the weight of Ag at 10.10% (Fig. 5(c)), while the weight of Ag estimated from the TGA results was 4.9%. The difference could be due to the inconsistent distribution of AgNPs within the film. The limitation of the diffusion of AgNPs into the BC fibril network resulted in lower concentration of AgNPs in the interior part as compared to the outer part of the film. Therefore, the actual average concentration of AgNPs in the film should be lower than the value reported from the EDX result. On the other hand, the weight (%) obtained from the TGA result was from the analysis of the entire film sample; therefore, the value was lower than that obtained from the EDX result.

### 3.5. Water Absorption

The sample of BC-SNR-0.08Ag was determined for water absorption capacity (WAC) and the WAC profile for 15 days immersion in deionized water is shown in Fig. 8. It was demonstrated that BC-SNR-0.08Ag can be considered as a material with high water adsorption capacity. After 15 days in deionized water, the WAC of BC-SNR-0.08Ag composites were 153%. The high WAC of BC is due to its porosity and large surface area, which physically traps water molecules both on the surface and within the interconnected fibrils of the BC networks. The very high porosity of BC promotes its WAC of the BC-SNR-Ag composite by providing a large surface area and high pore volume that allow it to absorb and retain substantial amounts of water [34]. Additionally, hydrogen bonding facilitates the binding of water molecules to the BC fibrils [35]. For a comparison, the WAC of BC was about 700% in the first 4 days; afterwards, the water absorption only increases slightly to a saturation of ~ 800% after 16 days [17]. On the other hand, the SNR film showed a much lower WAC of 40% over 16 days [17]. The water absorption rate of BC-SNR-Ag film was relatively high in the first 24 hours. After that, the water absorption gradually increased with time and reached 153% after 15 days, which was about four times that of the SNR film. However, it still did not reach equilibrium within 15 days. The significantly reduced WAC and much lower water absorption rate as compared to that of the pure BC film was due to the denser structure filled with hydrophobic polymer of SNR. In addition, it was also reported that the incorporation of AgNPs in BC matrix could also lower the porosity of the film; thereby reducing water penetration and WAC of the film [30]. The WAC of natural rubber/cellulose fiber cellulose film was found slightly dropped after adding silver nanoparticles, but remained

high values resulted from the cellulose microfibril reinforcement [36].

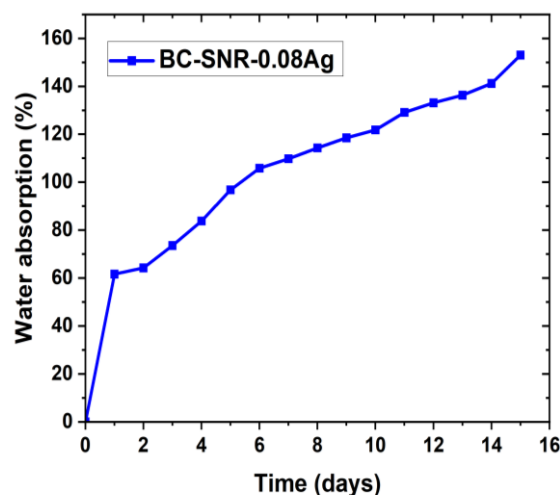


Fig. 8. Water absorption capacity (WAC) of BC-SNR-0.08Ag composite film.

### 3.6. Antibacterial Properties

The composite film of BC-SNR-0.08Ag was evaluated for its antibacterial properties as shown in Fig. 9. For antibacterial activity evaluation, *S. aureus* and *E. coli* were selected to represent gram-positive and gram-negative bacteria, respectively.

The film of BC-SNR exhibited an increase in bacterial growth for both gram-positive and gram-negative strains. This increase might be due to smaller particles such as proteins, lipids, and carbohydrates present in SNR that were integrated into BC film [37]. On the other hand, the film of BC-SNR-0.08Ag, which contains AgNPs, showed excellent antibacterial properties, reducing *S. aureus* by nearly 98% and *E. coli* by 63%.

AgNPs have a broad-spectrum antibacterial effect, targeting both gram-positive and gram-negative bacteria, thus effectively addressing a wide range of bacterial pathogens. The antibacterial effectiveness of AgNPs is likely due to their ability to disrupt the cell membrane. Furthermore, the small size and high surface area-to-volume ratio of these nanoparticles enhance their interaction with bacterial cells [36, 38, 39]. The integration of AgNPs into the BC-SNR film promoted antibacterial properties by embedding AgNPs in BC-SNR matrix, which effectively interacted with bacteria.

## 4. Conclusion

In this study, the successful synthesis of BC-SNR-Ag composite films resulted in notable enhancements in advantageous properties such as flexibility and antibacterial properties. AgNPs were successfully synthesized using the reduction reaction of  $\text{AgNO}_3$ , and functional groups in the stabilizing agent in SNR latex. The synthesis of BC-SNR-Ag composite was achieved by immersing BC pellicle in the suspension of Ag-SNR.



Compared to pure BC, the composite film of BC-SNR-0.08Ag exhibited a considerably higher value of strain at break at about 14%. The inclusion of AgNPs significantly enhanced antibacterial properties of the composites. The composite films exhibit high thermal stability, water absorption properties, and good mechanical strength. Their enhanced thermal resistance ensures durability under high-temperature conditions, while the high-water absorption capacity and robust mechanical properties provide reliability and versatility. Due to their enhanced properties, the developed BC-SNR-Ag composite films have potential applications for flexible electronics, such as a semiconductor film for moisture detection, which could lead to the development of highly efficient and affordable moisture sensors, making it a promising candidate for widespread use. Further study of its applications has been in process.

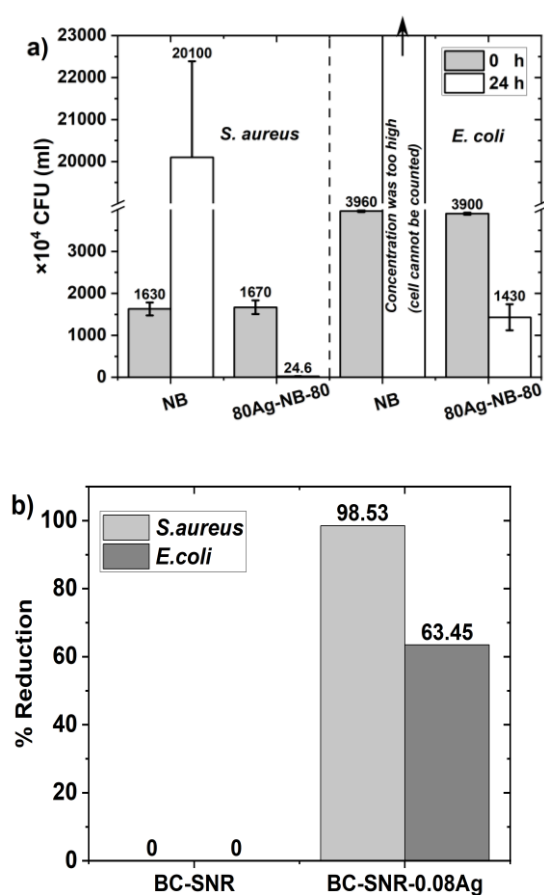


Fig. 9. Antibacterial properties of BC-SNR-0.08Ag composite film against *Staphylococcus aureus* (*S.aureus*) and *Escherichia coli* (*E.coli*): (a) A colony forming unit (CFU) and (b) %reduction.

## Acknowledgement

This research is funded by Thailand Science Research and Innovation Fund, Chulalongkorn University (No. 6641/2566).

## References

- [1] W. Smitthipong, "Cream concentrated latex for foam rubber products," in *4th International Conference on Mechanical, Materials and Manufacturing (ICMMM 2017)*, Atlanta, USA, 2017, vol. 272, doi: 10.1088/1757-899X/272/1/012025.
- [2] J. K. Igbo, L. O. Chukwu, E. O. Oyewo, and J. L. Blum, "The chemistry and health outcomes of electronic waste (E-Waste) leachate: Exposure to E-Waste is toxic to Atlantic Killifish (*Fundulus heteroclitus*) embryos," *Sustainability*, vol. 14, no. 18, 2022, doi: 10.3390/su141811304.
- [3] J. T. McNamara, J. L. W. Morgan, and J. Zimmer, "A molecular description of cellulose biosynthesis," *Annu. Rev. Biochem.*, vol. 84, pp. 895–921, 2015, doi: 10.1146/annurev-biochem-060614-033930.
- [4] X. Li, C. Ding, X. Li, H. Yang, and S. Liu, "Electronic biopolymers: From molecular engineering to functional devices," *J. Chem. Eng.*, vol. 397, p. 125499, 2020, doi: 10.1016/j.ccej.2020.125499.
- [5] A. M. Díez-Pascual, "Synthesis and applications of biopolymer composites," *Int. J. Mol. Sci.*, vol. 20, no. 9, p. 2321, 2019, doi: 10.3390/ijms20092321.
- [6] M. P. Bartolomé, A. Mora-Boza, and L. G. Fernández, "Emerging biofabrication techniques: A review on natural polymers for biomedical applications," *Polymers-Basel*, vol. 13, no. 8, 2021, doi: 10.3390/polym13081209.
- [7] P. Jittaut, P. Hongsachart, S. Audtarat, and T. Dasri, "Production and characterization of bacterial cellulose produced by *Gluconacetobacter xylinus* BNKC 19 using agricultural waste products as nutrient source," *Arab j. basic appl. sci.*, vol. 30, no. 1, pp. 221-230, 2023, doi: 10.1080/25765299.2023.2172844.
- [8] Q. L. Lu, J. Wu, Y. Yi, L. Li, and B. Huang, "One-pot green extraction of high charge density cellulose nanocrystals with high yield for bionanocomposites," *J. Mater. Sci.*, vol. 56, no. 1, pp. 12212-12223, 2021, doi: 10.1007/s10853-021-06085-9.
- [9] R. Mehrotra, S. Sharma, N. Shree, and K. Kaur, "Bacterial cellulose: An ecological alternative as a biotextile," *Biosciences Biotechnology Research Asia*, vol. 20, no. 2, pp. 449-463, 2023, doi: 10.13005/bbra/3101.
- [10] V. Kitsawat, S. Siri, and M. Phisalaphong, "Electrically conductive natural rubber composite films reinforced with graphite platelets," *Polymers*, vol. 16, no. 2, 2024, doi: 10.3390/polym16020288.
- [11] W. B. Sun, Z. M. Han, X. Yue, H. Y. Zhang, K. P. Yang, and Z. X. Liu, "Nacre-inspired bacterial cellulose/mica nanopaper with excellent mechanical and electrical insulating properties by biosynthesis," *Adv. Mater.*, vol. 35, no. 24, 2023, doi: 10.1002/adma.202300241.
- [12] M. P. Raut, E. Asare, S. M. Daniel, E. N. Amadi, and I. Roy, "Bacterial cellulose-based blends and composites: Versatile biomaterials for tissue

- engineering applications,” *Int. J. Mol. Sci.*, vol. 24, no. 2, p. 986, 2019, doi: 10.3390/ijms24020986.
- [13] Y. Wang, S. Lu, W. He, S. Gong, and Y. Zhang, “Modeling and characterization of the electrical conductivity on metal nanoparticles/carbon nanotube/polymer composites,” *Scientific Reports*, vol. 12, no. 10448, 2022, doi: 10.1038/s41598-022-14596-x.
- [14] Z. Wu, S. Chen, J. Li, B. Wang, and M. Jin, “Insights into hierarchical structure–property–application relationships of advanced bacterial cellulose materials,” *Adv. Funct. Mater.*, vol. 33, no. 12, 2023, doi: 10.1002/adfm.202214327.
- [15] P. Danwanichakul and B. Than-ardna, “Permeation of salicylic acid through skim natural rubber films,” *Industrial Crops and Products*, vol. 122, pp. 166-173, 2018, doi: 10.1016/j.indcrop.2018.05.066.
- [16] N. Lehman, A. Tuljitrarnorn, L. Songtipya, N. Uthaipan, and K. Sengloyluan, “Influence of non-rubber components on the properties of unvulcanized natural rubber from different clones,” *Polymers*, vol. 14, no. 9, 2022, doi: 10.3390/polym14091759.
- [17] P. Sintharm, A. Nimpaboon, Y. C. Liao, and M. Phisalaphong, “Bacterial cellulose reinforced with skim/fresh natural rubber latex for improved mechanical, chemical and dielectric properties,” *Cellulose*, vol. 29, no. 4, pp. 1-20, 2022, doi: 10.1007/s10570-021-04366-9.
- [18] H. S. M. Sajith, R. Sulthan, and S. Sambhudevan, “Natural rubber and gutta-percha rubber,” in *Handbook of Biopolymers*. 2023, pp. 1-35, doi: 10.1007/978-981-16-6603-2\_30-1.
- [19] N. Jirasitthanita and P. Danwanichakul, “Liquid-phase exfoliation of graphite using the serum from skim natural rubber latex,” *Eng. J.*, vol. 27, no. 5, 2023, doi: 10.4186/ej.2023.27.5.37.
- [20] M. Pinitjitsamuta and P. Doungmanee, “Assessing the impact of rubber development policies on the national economy, intro-sector dynamics, and employment: utilizing a computable general equilibrium model approach,” *RMUTT global business accounting and finance review*, vol. 8, no. 1, pp. 68-84, 2024, doi: 10.60101/gbafr.2024.271025.
- [21] H. Salsabila, M. Antoni, and D. Adriani, “Trend TSR 20 rubber prices between producing countries in Southeast Asia,” *N.a. J. Adv. Res. Rev.*, vol. 23, no. 1, pp. 1466-1471, 2024, doi: 10.30574/wjarr.2024.23.1.2078.
- [22] Wahyudiono, S. Machmudah, H. Kanda, Y. Zhao, and M. Goto, “Pulsed discharge plasma in slug-flow reactor system for water pollutant removal and nanoparticle synthesis,” *Eng. J.*, vol. 25, no. 9, 2021, doi: 10.4186/ej.2021.25.9.1.
- [23] V. Poli and S. R. Motireddy, “Review on synthesis and applications of silver nanoparticles, their characterization and toxicity effects: future outlook,” *Int. J. Food. Sci. Nutr.*, vol. 9, no. 173, 2023, doi: 10.24966/FSN-1076/100173.
- [24] T. Suwatthanarak, B. Than-ardna, D. Danwanichakul, and P. Danwanichakul, “Synthesis of silver nanoparticles in skim natural rubber latex at room temperature,” *Mater. Lett.*, vol. 168, pp. 31-35, 2016, doi: 10.1016/j.matlet.2016.01.026.
- [25] P. Danwanichakul, T. Suwatthanarak, C. Suwanvisith, and D. Danwanichakul, “The role of ammonia in synthesis of silver nanoparticles in skim natural rubber latex,” *J. Nanosci.*, vol. 2016, 2016, doi: 10.1155/2016/7258313.
- [26] T. Suratago, P. Panitchakarn, P. Kerdlarpphon, N. Rungpeerapong, V. Burapatana, and M. Phisalaphong, “Bacterial cellulose-alginate membrane for dehydration of biodiesel-methanol mixtures,” *Eng. J.*, vol. 20, no. 5, 2016, doi: 10.4186/ej.2016.20.5.145.
- [27] B. Villa, E. García, M. Pradena, P. Flores, and C. Medina, “Surface modification of rubber from end-of-life tires for use in concrete: A design of experiments approach,” *J. Chil. Chem. Soc.*, vol. 65, no. 4, 2020, doi: 10.4067/S0717-97072020000404988
- [28] P. J. Li, J. J. Pan, L. J. Tao, X. Li, and D. L. Su, “Green synthesis of silver nanoparticles by extracellular extracts from *Aspergillus Japonicus* PJ01,” *Molecules*, vol. 26, no. 15, 2021, doi: 10.3390/molecules26154479.
- [29] A. A. Tehrani, M. M. Omranpoor, A. Vatanara, M. Seyedabadi, and V. Ramezanicorresponding, “Formation of nanosuspensions in bottom-up approach: theories and optimization,” *DURA Journal of Pharmaceutical Sciences*, vol. 27, no. 1, pp. 451-473, 2019, doi: 10.1007/s40199-018-00235-2.
- [30] R. Jenkhongkarn and M. Phisalaphong, “Effect of reduction methods on the properties of composite films of bacterial cellulose-silver nanoparticles,” *Polymers*, vol. 15, 2023, doi: 10.3390/polym15142996.
- [31] O. Ş. A. Koroğlu, I. Kürkçüoğlu, D.Ö. Dede, T. Özdemir, B. Hazer, “Silver nanoparticle incorporation effect on mechanical and thermal properties of denture base acrylic resins,” *J. Appl. Oral. Sci.*, vol. 24, no. 6, pp. 590-596, 2016, doi: 10.1590/1678-775720160185.
- [32] K. Potivara and M. Phisalaphong, “Development and characterization of bacterial cellulose reinforced with natural rubber,” *Materials*, vol. 12, no. 14, p. 2323, 2019, doi: 10.3390/ma12142323.
- [33] L. C. Yeng, M. U. Wahit, and N. Othman, “Thermal and flexural properties of regenerated cellulose(RC)/poly(3-hydroxybutyrate)(PHB)biocomposites,” *Latest Research Development in Mechanical Engineering*, vol. 75, no. 11, pp. 107-112, 2015, doi: 10.11113/jt.v75.5338.
- [34] K. Gelin, A. Bodin, P. Gatenholm, A. Mihranyan, K. Edwards, and M. Strømme, “Characterization of water in bacterial cellulose using dielectric spectroscopy and electron microscopy,” *Polymers*, vol. 48, no. 26, pp. 7623-7631, 2007, doi: 10.1016/j.polymer.2007.10.039.

- [35] N. B. Khandoker Samaher Salem , Hasan Jameel , Lokendra Pal , Lucian Lucia “Computational and experimental insights into the molecular architecture of water-cellulose networks,” *Matter*, vol. 6, no. 5, pp. 1366-1381, 2023, doi: 10.1016/j.matt.2023.03.021.
- [36] G. Supanakorn, S. Taokaew, and M. Phisalaphong, “Multifunctional cellulosic natural rubber and silver nanoparticle films with superior chemical resistance and antibacterial properties,” *Nanomaterials*, vol. 13, no. 521, 2023, doi: doi.org/10.3390/nano13030521.
- [37] W. H. Hoover and S. R. Stokes, “Balancing carbohydrates and proteins for optimum rumen microbial yield,” *Journal of Dairy Science*, vol. 74, no. 10, pp. 3630-3644, 1991, doi: 10.3168/jds.S0022-0302(91)78553-6.
- [38] K. Zawadzka, K. Kądziola, A. Felczak, N. Wrońska, and I. Piwoński, “Surface area or diameter – which factor really determines the antibacterial activity of silver nanoparticles grown on TiO<sub>2</sub> coatings?,” *New Journal of Chemistry*, vol. 38, pp. 3275-3281, 2014, doi: 10.1039/C4NJ00301B.
- [39] S. Khorrami, A. Zarrabi, M. Khaleghi, M. Danaei, and M. R. Mozafari, “Selective cytotoxicity of green synthesized silver nanoparticles against the MCF-7 tumor cell line and their enhanced antioxidant and antimicrobial properties,” *Int J Nanomedicine*, vol. 13, p. 8013—8024, 2018, doi: 10.2147/IJN.S189295.



**Puttakhun Meemai**, photograph and biography not available at the time of publication.

**Theerapart Sripetchdanon**, photograph and biography not available at the time of publication.

**Nuntaporn Laosarakham**, photograph and biography not available at the time of publication.

**Saranrat Siri**, photograph and biography not available at the time of publication.

**Adun Nimpaiboon**, photograph and biography not available at the time of publication.

**Muenduen Phisalaphong**, photograph and biography not available at the time of publication.